(This is a sample cover image for this issue. The actual cover is not yet available at this time.)

Journal of Electrostatics 71 (2013) 48–52

Contents lists available at SciVerse ScienceDirect

Journal of Electrostatics

journal homepage: www.elsevier.com/locate/elstat

Structural, optical and electrical properties of tin oxide thin films by electrostatic spray deposition

Bhavana N. Joshi, Hyun Yoon, Sam S. Yoon*

School of Mech. Eng., Korea University Anam-Dong, Seongbuk-Gu, Seoul 136-713, Republic of Korea

ARTICLE INFO

Article history:
Received 3 July 2012
Received in revised form
10 October 2012
Accepted 21 November 2012
Available online 3 December 2012

Keywords:
Electrostatic spray deposition
SnO_2
Electrical resistivity

ABSTRACT

Tin oxide (SnO_2) thin films were deposited by electrostatic spray deposition (ESD). The structural, optical and electrical properties of the films for different solvents were studied. The morphology of the deposited thin films was investigated by scanning electron microscopy. The optical transmission spectra of the films showed 66–75% transmittance in the visible region of spectrum. The electrical resistivity of thin films deposited using the different solvents ranged 1.08×10^{-3}–1.34×10^{-3} Ω-cm. Overall, EG and PG were good solvents for depositing SnO_2 thin films by the ESD technique with stable cone jet.

1. Introduction

Transparent conducting oxide (TCO) thin films have been extensively studied and have wide variety of technological applications in photovoltaic cells and optoelectronics because of coexistence of low resistivity and high optical transparency in visible range of solar spectrum. Tin Oxide (SnO_2) thin films with stability in atmospheric conditions, chemical inertness, mechanical hardness and high temperatures resistance, is the most popular among the available transparent conducting oxides. SnO_2 has a wide bandgap, transparency to visible light and *n*-type conduction properties [1]. The oxygen deficiency in SnO_2 makes it a conductive material. Thin films of SnO_2 have been widely used as front electrodes in solar cells and flat-panel displays, smart windows, phototransistors as well as IR heat mirrors, low emissive windows, etc [2].

Many technological methods for depositing SnO_2 thin films has been investigated, such as magnetron sputtering [3], sol–gel [4], chemical vapor deposition [5], spray [6], and electrostatic spray deposition(ESD) [7]. With these techniques, thin films of different thicknesses, surface morphologies, crystal sizes, electrical and optical properties can be deposited. The ESD technique, which is simple and cost-effective, can work with a wide range of precursors. The main advantages of the ESD method are that it produces fine, uniform, self-dispersive and highly wettable atomized droplets, thereby reducing material consumption with little waste. In ESD, the precursor solution is atomized to an aerosol by an applied electric field between the metal capillary and the grounded substrate, on which the thin film is deposited. The precursor solution can be atomized in different spray modes depending on the applied voltage, and the flowrate and physical properties of the precursor. Various spraying modes have been discussed [8,9]. Basically these modes are classified into two major categories, the dripping mode and the spray mode, which includes the cone jet mode. The cone jet mode is most often used in thin film deposition to obtain uniform thin films.

Matsushima et al. [10] deposited SnO_2 thin films by ESD using $SnCl_2$ and ethanol on a Au-coated Pyrex glass substrate at 773 K. The deposition of amorphous SnO_2 films on Nickel substrates using $SnCl_4 \cdot 5H_2O$ and ethanol mixture by ESD were reported by Mohamedi et al. [11] for their uses in lithium batteries as an anode material. Culha et al. [4] used the sol–gel dip coating method for the synthesis of SnO_2 thin films using combination of $SnCl_2$, glacial acetic acid and methanol for gas sensing applications. More recently, Yu et al. [12] prepared SnO_2 films on Ni foam and foil at 250 °C by ESD using tin acetate dissolved in ethanol and ethylene glycol solvent. According to these literature, ethanol is a common solvent for the deposition of SnO_2 while taking advantage of ESD.

Most importantly, the solvent must yield a stable cone-jet during ESD. The thermo-physical properties of the solvents, such as liquid's relative permittivity, surface tension, viscosity and density, have a prominent influence on the cone-jet stability. Per Eq. (1) [13–16], the diameter, flowrate, and current of the cone-jet

* Corresponding author.
E-mail address: skyoon@korea.ac.kr (S.S. Yoon).

0304-3886/$ – see front matter © 2012 Elsevier B.V. All rights reserved.
http://dx.doi.org/10.1016/j.elstat.2012.11.024

generated by electrostatic atomization are mainly dependent on the electrical permittivity in vacuum (ε_0), surface tension (γ), density (ρ), electrical conductivity (K), relative dielectric constant (or relative permittivity, κ) of the solution:

$$d_0 \approx \left[\gamma\varepsilon_0^2/(\rho K^2)\right]^{1/3}$$
$$Q_0 \approx \gamma\varepsilon_0/(\rho K) \quad (1)$$
$$I_0 \approx \left(\gamma^2\varepsilon_0/\rho\right)^{1/2}$$

The viscosity of the solvent also has an important effect on the stabilization of the cone jet, whose stability is a prerequisite to obtaining good quality thin films. After several experiments using different solvents, ethylene glycol (EG), propylene glycol (PG) and their mixtures with iso-propyl alcohol (PA) are observed to yield stable cone jets for longer durations. Thus, the aim of this study is to investigate the effect of these solvents on the structural, optical, morphological and electrical properties of SnO_2 thin films.

An indium tin oxide (ITO) substrate is used to meet the requirement of using a conducting substrate in the ESD technique. The literature survey shows that the transparent conducting substrate works as a current collector and a semiconductor support. The indium tin oxide (ITO) is a *n*-type semiconductor material widely used for fabricating transparent conducting substrates used in dye synthesized solar cells (DSSC). The sheet resistance of the substrate significantly increases when it is annealed at a temperature higher than 300 °C. The DSSCs using an ITO substrate have low efficiency due to the energy losses resulting from the increase in substrate resistivity. Ngamsinlapasathian et al. [17] and Yoo et al. [18] used ITO/SnO_2 and ITO/FTO (fluorine doped tin oxide) double layered TCOs in DSSCs, respectively, to improve heat stability by preventing the loss of oxygen vacancies from the ITO.

2. Experimental

The precursors are prepared by dissolving 0.05 M $SnCl_4 \cdot 5H_2O$ with EG + PA, EG and PG separately as shown in Table 1. The volume ratio of EG:PA was set to 1:1. After the addition of $SnCl_4 \cdot 5H_2O$ to the aforementioned solvents, the mixed precursors were magnetically stirred for 5 min for its complete dissolution. The precursors were then sprayed by using a nozzle of 4 mm diameter on pre-cleaned 2×1 cm^2 ITO glass substrates kept at 70 °C to induce evaporation of the solvents. Here, the solvents refer to EG, PG, and PA, while the precursors refer to the mixtures of solvents and $SnCl_4 \cdot 5H_2O$. The schematic of the ESD setup (shown in Fig. 1) used for thin film deposition is discussed in detail elsewhere [9]. The ITO coated substrates ($\rho = 2.1 \times 10^{-4}$ Ω-cm) were used because the substrate needed to be a conducting material to facilitate charge grounding for the ESD system. The downward facing nozzle center was aligned with the plate separated by a 30 mm gap. The precursor issued from a syringe pump at a flowrate adjusted to yield a stable Taylor cone-jet, thereby producing the smallest droplets possible under the given operating conditions. A voltage-supply wire was attached to the charging needle (i.e., anode connected to a higher potential), and the substrate (i.e., cathode) was grounded. The experiment was repeated at least 3–4 times to confirm the repeatability of film production and thus the reliability of our data. Finally, all of the films were annealed in oven in air ambience at 500 °C for 1 h.

Table 1
Optimized process parameters for yielding stable cone-jet mode of electrospray.

Solvents	Solvent proportion [mL:mL]	Flowrate [μL/hr]	Applied voltage [kV]
Ethylene glycol + iso-propyl alcohol (EG + PA)	25:25	15	13.3
Ethylene glycol (EG)	50	25	14.4
Propylene glycol (PG)	50	40	12.8

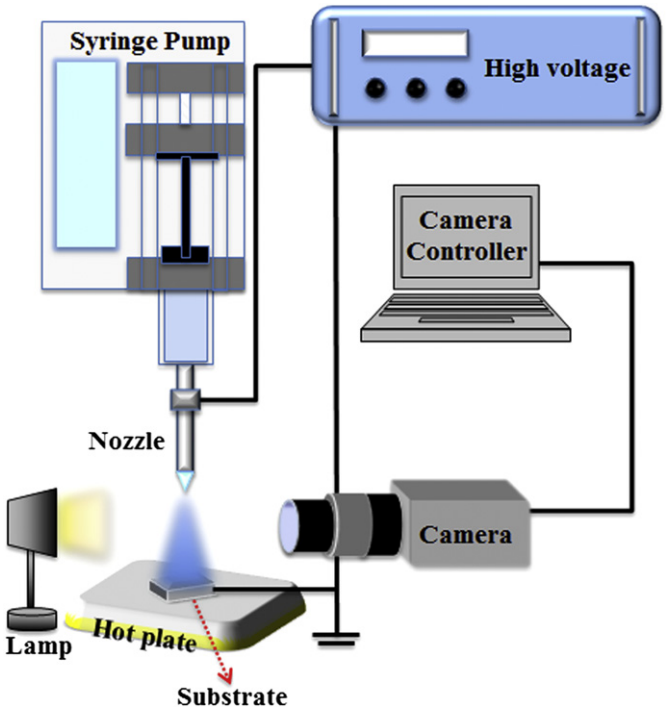

Fig. 1. ESD Schematics.

Conductivity, viscosity and surface tension of the precursors were determined prior to the deposition of the thin films. Surface morphology and thickness of the films were measured and analyzed from surface and cross-sectional views by using a scanning electron microscope (HRSEM, Philips, XL30SFEG at 10 kV). The non-contact mode atomic force microscope (AFM Park Systems Xe-100) was utilized to measure the root mean square (RMS) and the average roughness of the films. The structural properties of the films were determined by using X-ray diffraction (XRD, Rigaku Japan, D/MAX-2500). The transmittance and bandgap of the films were studied by a UV visible spectrometer (4974 SPEC – Unicam UV-530). Hall device (Ecopia HMS-3000) was used to study the current voltage (*IV*) curve and electrical properties of the SnO_2 thin films.

3. Results and discussion

The properties of synthesized precursors determined through various characterizations are presented in Table 2. As in Eq. (1), the higher the conductivity, the smaller the droplet size will be. Thus, EG + PA and EG precursors having high conductivity are expected to produce smaller droplets than the PG-based precursors. The

Table 2
Properties of solvents.

Solvents/Precursors		Surface tension [mN/m]	Conductivity [μS/cm]	Viscosity [mPa·s]	Boiling point [C]
Pure solvents	PA	21.8	3.5	2.4	82.5
	EG	48.4	0.3	21	197.3
	PG	40.1	0.1	56	188.2
Sn precursors	EG + PA	23	183	6.7	Unknown
	EG	47.3	342	21	Unknown
	PG	42.8	58	56	Unknown

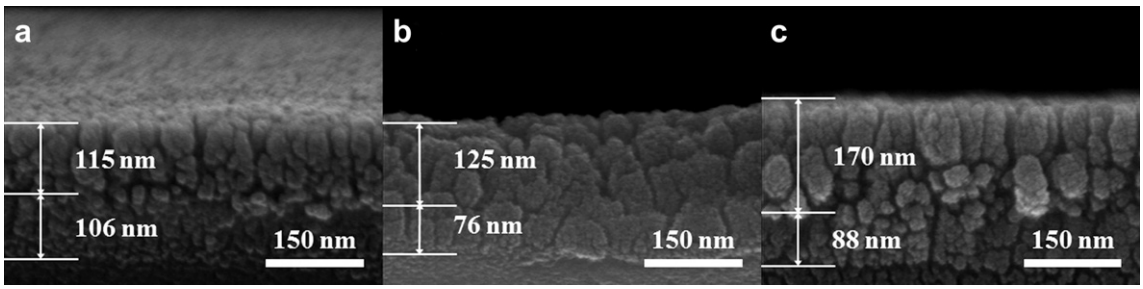

Fig. 2. SEM images showing the thickness of the annealed films deposited for 1 h spraying. The solvents used were (a) EG + PA, (b) EG, and (c) PG. Thickness of the ITO substrates ranged from 76 to 106 nm.

conductivities of iso-propyl alcohol (PA), ethylene glycol (EG) and propylene glycol (PG) changed drastically from their conductivities in pure form after the addition of $SnCl_4 \cdot 5H_2O$. The viscosities and surface tensions of EG and PG were not greatly influenced by the addition of $SnCl_4 \cdot 5H_2O$. PA was mixed with EG to make another type of solvent. Various precursor choices are expected to yield different structural, electrical, and optical characteristics of SnO_2 thin films; it would be informative to investigate their characteristics. The surface tension and viscosity of the precursor were changed significantly after mixing EG with PA, as shown in Table 2. The viscosity is high for PG and EG. The flowrate that yielded a stable cone-jet mode was high for the PG-based precursors because of their relatively low conductivity. On the other hand, the flowrate of EG-based precursors was low because their conductivity increased with the addition of $SnCl_4 \cdot 5H_2O$.

The thickness of the films was determined from the cross-sectional SEM micrographs. Each sample was scanned at various places. The films were found to have uniform thickness. The typical cross-sectional SEM images of SnO_2 films with different thicknesses due to the different solvents used are shown in Fig. 2. The thickness of the films was largest for solvent PG; $t = 170$ nm. The EG + PA precursor having lower viscosity, surface tension and conductivity than the EG precursor gave a stable cone jet at very small flowrate, consequently affecting on thickness of thin film. The SEM surface views of the thin films with different solvent precursors are shown in top row in Fig. 3. The surfaces of the thin films of the EG based precursors show a formation of platelet like structures whereas the surfaces of the thin films of the PG based precursors show a formation of granular particles. The 3D view of AFM of the films presented in bottom row in Fig. 3 clearly shows the uniformity of films similar to the results of the SEM. The RMS and average roughness values were determined from the XEI data processing analysis software available with the AFM system. The RMS and average roughness values of the films are presented in Table 3. The results show that the higher viscosity solvents gave a smoother surface morphology. The average roughness of the ITO substrate was 0.37 nm.

Fig. 4 illustrates the XRD pattern of the SnO_2 thin films deposited using various solvents. The broad and weak peaks of the SnO_2 films deposited using PG indicate the polycrystalline phase whereas in the case of SnO_2 films using EG and EG + PA precursors, the intensities of the peaks are very low. The peaks of (110), (101) and (200) planes correspond to diffraction angle (2θ), 26.8°, 33.9°, and 37.1° respectively; this confirms SnO_2 formation. The presence of other orientations such as (101), (211) and (310) was also detected with a slight change in 2θ position because of the overlapping of the SnO_2 thin films and the ITO substrate. The interplanar distance d was observed to be in agreement with d value mentioned in JCPDS file No. 41-1445.

The transmittance spectra of the annealed SnO_2 films deposited on ITO substrates using different solvents were recorded in the wavelength range of 330–800 nm as shown in Fig. 5. The EG based SnO_2 thin films show better transmittance than the PG based SnO_2 thin films; however, as expected, all the films show lower

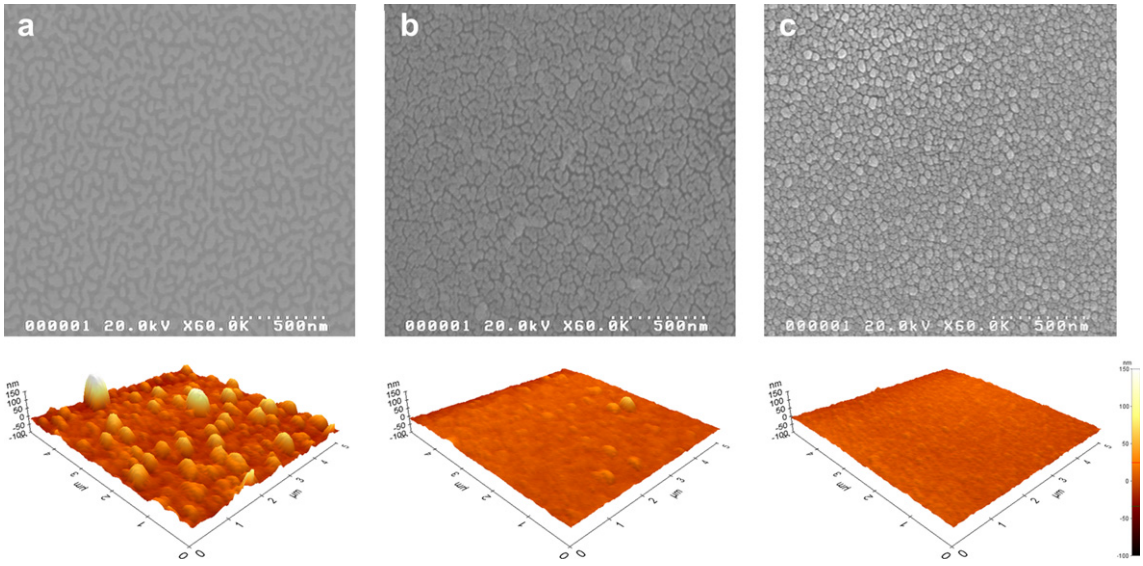

Fig. 3. The top SEM and bottom AFM images show the surface morphology of the SnO_2 films deposited by using various solvents, as (a) EG + PA, (b) EG, and (c) PG.

Table 3
Roughness of films determined by AFM.

Precursor	Roughness [nm]	
	RMS	Average
EG + PA	6.652	5.115
EG	1.452	1.029
PG	1.274	1.009

Table 4
Effect of variation in solvent electrical and optical properties.

Sample	ρ [$\times 10^{-3}$ Ω-cm]	σ [S/cm]	μ [cm^2/V-s]	n_e [$\times 10^{19}$ cm^{-3}]	FOM [$\times 10^{-3}$ Ω^{-1}]	E_g [eV]
ITO	0.21	4694	48.2	−60.74	–	3.50
EG + PA	1.12	896	51.3	−10.9	6.7	3.52
EG	1.08	925	49.3	−11.7	7.9	3.54
PG	1.34	725	49.6	−9.38	6.7	3.54

transmittance than the ITO substrate. The absorption edges of all thin films are shifted to higher wavelengths with respect to that of ITO. This shift is due to the decrease in carrier concentration, which lowers the Fermi level and reduces the magnitude of the Burstein effect. These films became more transparent than the as-deposited films after high temperature annealing because of enhanced grain growth. The films deposited using the EG + PA and EG precursor solvents show average transmittance of about 70% and 75% whereas, the films using the PG based precursor solvent show average transmittance of 66.26%. The absorption coefficient (α), which corresponds to electron excitation from the valance band to conduction band, is used to determine the nature and value of the optical bandgap using the Beer–Lambert's law [19], $\alpha = (1/t)\log(1/T)$, where, t is a thickness and T is transmittance of the film.

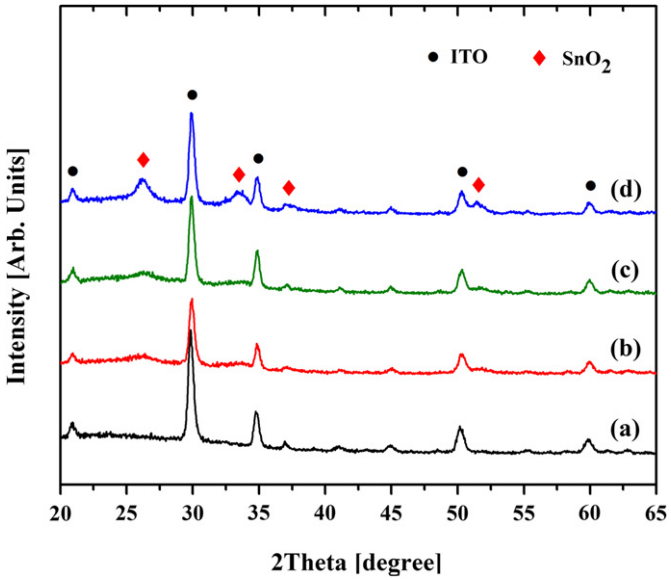

Fig. 4. The XRD pattern of (a) the ITO substrate and annealed films deposited using (b) EG + PA, (c) EG and (d) PG based precursors.

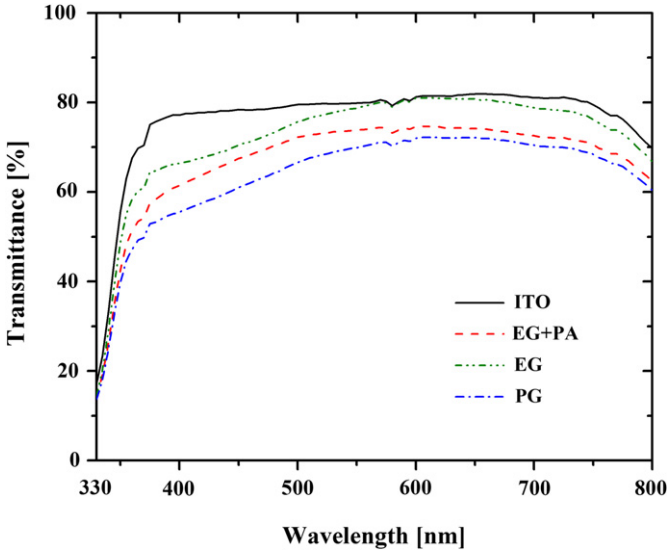

Fig. 5. The transmittance spectra of the ITO substrate and annealed films deposited by using different solvents.

The optical bandgaps (E_g) of the SnO_2 films and ITO substrate for different solvents presented in Table 4 were determined by extrapolating the linear portion of the $(\alpha h\nu)^2$ vs. $h\nu$ plots. The bandgap of the ITO coated glass is 3.5 eV. The bandgaps of the SnO_2 thin films deposited on ITO range from 3.52 to 3.54 eV. These bandgap values are in agreement with the bandgap values of SnO2 thin films (3.38–3.58 eV) deposited on glass substrates by Amma et al. [20] using the $SnCl_4{\cdot}5H_2O$ precursor by the spray pyrolysis technique.

The electrical properties such as I–V characteristics, resistivity (ρ), conductivity (σ), mobility (μ) and carrier concentration (n_e) of the SnO_2/ITO bilayer were measured using a Hall set up with the Van der Pauw method. For these measurements, indium contacts were applied to the four corners of the SnO_2 thin films. The total thickness of the bilayer, i.e. the thickness of the SnO_2 film and the ITO substrate, was used in the Hall measurements. Fig. 6 shows the I–V characteristics of the SnO_2 films. The straight line I–V curve indicates the Ohmic nature of the thin films. The sheet resistance of our films increased by two fold for the SnO_2/ITO bilayer than for the pure ITO (21 Ω/□). On the other hand, Ngamsinlapasathian et al. [21] showed that the SnO_2/ITO bilayer deposited by RF magnetron sputtering had the sheet resistance of 6.9 Ω/□, which is similar to that of pure ITO substrate (6.3 Ω/□). This sheet resistance difference is attributed to the differences in deposition techniques and precursors' thermo-physical properties. Table 4 shows the effect of

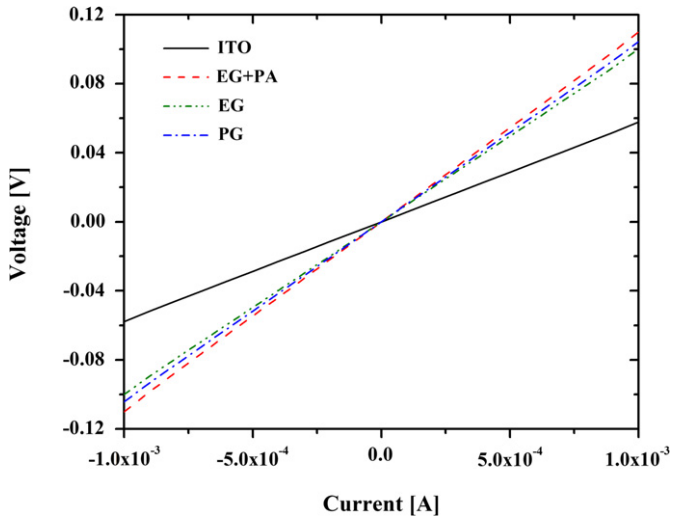

Fig. 6. I–V characteristics of the annealed films fabricated by using different solvents.

variation in solvent on the electrical properties of the SnO_2 thin films. The resistivity and carrier concentration of the SnO_2 thin films decrease more than those of ITO whereas the mobility slightly increases. The figure of merit (FOM) first defined by Haacke [22] is an important parameter for evaluating the performance of TCO thin films. FOM is directly proportional to transmittance and inversely proportional to sheet resistance and it should be maximized for effective usage of TCO films. Usually transmittance (T) is taken at $\lambda = 550$ nm because at this wavelength, solar power conversion is maximum [23]. The figure of merit ranged from 6.7×10^{-3} to $7.9 \times 10^{-3}\ \Omega^{-1}$ for the SnO_2 thin films deposited using the ESD technique.

4. Conclusion

We have fabricated for the first time transparent and conducting SnO_2 thin films by using the ESD technique. Structural, morphological, optical and electrical properties of the films were investigated for various solvents. The optical bandgap energy values of the SnO_2 thin films ranged from 3.52 to 3.54. To achieve a high flowrate, the PG-based precursors were found to be suitable because of their low conductivity and high viscosity. However, the figure of merit varied from 6.7×10^{-3} to $7.9 \times 10^{-3}\ \Omega^{-1}$ for the SnO_2 films deposited using EG and PG based precursors.

Acknowledgment

This study was supported by a grant from the cooperative R&D Program (B551179-08-03-00) funded by the Korea Research Council Industrial Science and Technology, Republic of Korea. This research was also supported by the Converging Research Center Program through the Ministry of Education, Science and Technology (2010K000969) and NRF-2012029433, NRF-2012-0001169, and NRF-2010-0010217.

References

[1] Z. Hu, J. Zhang, Z. Hao, Q. Hao, X. Geng, Y. Zhao, Highly efficient organic photovoltaic devices using F-doped SnO_2 anodes, Appl. Phys. Lett. 98 (2011) 123302.
[2] M.M. Bagheri-Mohagheghi, M. Shokooh-Saremi, The electrical, optical, structural and thermoelectrical characterization of *n*-and *p*-type cobalt-doped SnO_2 transparent semiconducting films prepared by spray pyrolysis technique, Phys. B Condens. Matter 405 (2010) 4205–4210.
[3] A.F. Khan, M. Mehmood, A. Rana, M. Bhatti, Effect of annealing on electrical resistivity of rf-magnetron sputtered nanostructured SnO_2 thin films, Appl. Surf. Sci. 255 (2009) 8562–8565.
[4] O. Culha, M. Ebeoglugil, I. Birlik, E. Celik, M. Toparli, Synthesis and characterization of semiconductor tin oxide thin films on glass substrate by sol–gel technique, J. Sol Gel Sci. Technol. 51 (2009) 32–41.
[5] Y. Matsushima, K. Maeda, T. Suzuki, Nature of dark-brown SnO_2 films prepared by a chemical vapor deposition method, J. Ceram. Soc. Jpn. 116 (2008) 989–993.
[6] D.P. Joseph, P. Renugambal, M. Saravanan, S.P. Raja, C. Venkateswaran, Effect of Li doping on the structural, optical and electrical properties of spray deposited SnO_2 thin films, Thin Solid Films 517 (2009) 6129–6136.
[7] D. Zaouk, Y. Zaatar, A. Khoury, C. Llinares, J.P. Charles, J. Bechara, Fabrication of tin oxide (SnO_2) thin film by electrostatic spray pyrolysis, Microelectron. Eng. 51–52 (2000) 627–631.
[8] A. Jaworek, A.T. Sobczyk, Electrospraying route to nanotechnology: an overview, J. Electrost. 66 (2008) 197–219.
[9] H. Yoon, J.H. Woo, Y.M. Ra, S.S. Yoon, H.Y. Kim, S. Ahn, J.H. Yun, J. Gwak, K. Yoon, S.C. James, Electrostatic spray deposition of copper–indium thin films, Aerosol Sci. Technol. 45 (2011) 1448–1455.
[10] Y. Matsushima, Y. Nemoto, T. Yamazaki, K. Maeda, T. Suzuki, Fabrication of SnO_2 particle-layer on the glass substrate using electrospray pyrolysis method and the gas sensitivity for H_2, Sens. Actuators B Chem. 96 (2003) 133–138.
[11] M. Mohamedi, S.J. Lee, D. Takahashi, M. Nishizawa, T. Itoh, I. Uchida, Amorphous tin oxide films: preparation and characterization as an anode active material for lithium ion batteries, Electrochim. Acta 46 (2001) 1161–1168.
[12] Y. Yu, L. Gu, A. Dhanabalan, C.H. Chen, C. Wang, Three-dimensional porous amorphous SnO_2 thin films as anodes for Li-ion batteries, Electrochim. Acta 54 (2009) 7227–7230.
[13] A. Ganan-Calvo, The size and charge of droplets in the electrospraying of polar liquids in cone-jet mode, and the minimum droplet size, J. Aerosol Sci. 25 (1994). 309–310.
[14] J. Rosell-Llompart, J. Fernandez de la Mora, Generation of monodisperse droplets 0.3 to 4 μm in diameter from electrified cone-jets of highly conducting and viscous liquids, J. Aerosol Sci. 25 (1994) 1093–1119.
[15] D.-R. Chen, D.Y.H. Pui, Experimental investigation of scaling laws for electrospraying: dielectric constant effect, Aerosol Sci. Technol. 27 (1997) 367–380.
[16] A.M. Gañán-Calvo, J. Dávila, A. Barrero, Current and droplet size in the electrospraying of liquids. Scaling laws, J. Aerosol Sci. 28 (1997) 249–275.
[17] S. Ngamsinlapasathian, T. Sreethawong, Y. Suzuki, S. Yoshikawa, Single-and double-layered mesoporous TiO_2/P25 TiO_2 electrode for dye-sensitized solar cell, Sol. Energy Mater. Sol. Cells 86 (2005) 269–282.
[18] B. Yoo, K. Kim, D.K. Lee, M.J. Ko, H. Lee, Y.H. Kim, W.M. Kim, N.G. Park, Enhanced charge collection efficiency by thin-TiO_2-film deposition on FTO-coated ITO conductive oxide in dye-sensitized solar cells, J. Mater. Chem. 20 (2010) 4392–4398.
[19] T. Ratana, P. Amornpitoksuk, S. Suwanboon, The wide band gap of highly oriented nanocrystalline Al doped ZnO thin films from sol–gel dip coating, J. Alloys Compd. 470 (2009) 408–412.
[20] D. Amma, V. Vaidyan, P. Manoj, Structural, electrical and optical studies on chemically deposited tin oxide films from inorganic precursors, Mater. Chem. Phys. 93 (2005) 194–201.
[21] S. Ngamsinlapasathian, T. Sreethawong, S. Yoshikawa, Enhanced efficiency of dye-sensitized solar cell using double-layered conducting glass, Thin Solid Films 516 (2008) 7802–7806.
[22] G. Haacke, New figure of merit for transparent conductors, J. Appl. Phys. 47 (1976) 4086–4089.
[23] S. Chacko, N. Sajeeth Philip, V. Vaidyan, Effect of substrate temperature on structural, optical and electrical properties of spray pyrolytically grown nanocrystalline SnO_2 thin films, Phys. Status Solidi (a) 204 (2007) 3305–3315.